

Color-octet scalars and potentially large CP violation at the LHC

Xiao-Gang He^{1,2}, German Valencia³ and Hiroshi Yokoya^{2,4*}

¹ *INPAC, Department of Physics, Shanghai Jiao Tong University, Shanghai, China*

² *Department of Physics, National Taiwan University, Taipei, Taiwan*

³ *Department of Physics, Iowa State University, Ames, IA 50011*

⁴ *National Center for Theoretical Sciences,
National Taiwan University, Taipei, Taiwan*

(Dated: May 21, 2018)

Abstract

We consider the phenomenology of CP violation in a color-octet extended scalar sector for $t\bar{t}$ production and decay at the LHC. In particular we study the effect of the two neutral color-octet scalars S_I and S_R that occur in the model. There are two new sources of CP violation: a phase in the couplings of $S_{I,R}$ to top-quarks; and two phases in the quartic couplings of the scalar potential. In resonant production of a single $S_{I,R}$ followed by its decay into $t\bar{t}$ pairs through the parton level process $gg \rightarrow S_{I,R} \rightarrow t\bar{t}$, we find large raw CP asymmetries which can reach 12%. These raw asymmetries are, of course, diluted by standard model (SM) $t\bar{t}$ pairs making observation of CP violation contingent on whether the resonance itself can be extracted from the SM background.

*Electronic address: hexg@phys.ntu.edu.tw, valencia@iastate.edu, hyokoya@hep1.phys.ntu.edu.tw

I. INTRODUCTION

Violation of charge-parity (CP) symmetry beyond the standard model (SM) has yet to be observed but we suspect that it must be there in order to explain the baryon asymmetry of the universe. This gives paramount importance to new searches for CP violation in high-energy frontier. One tool, proposed many years ago, for searches in collider experiments is the use of triple-product correlations [1], which are simple kinematic correlations of the form $\vec{p}_1 \cdot (\vec{p}_2 \times \vec{p}_3)$. These correlations are referred to as “naive- T ” odd because they reverse sign under the “naive- T ” operation that reverses the direction of momenta and spin without interchanging initial and final states. In general, correlations of this form can be CP even or CP odd, as they are induced by either loop level unitarity phases or by CP violating phases respectively. In top-quark pair production, these triple-product correlations originate in CP violating spin correlations with the top-quark (and anti-quark) weak decay acting as spin analyzer.

There exist several recent proposals to search for CP violation at the LHC using triple-product correlations. Our discussion is based on observables discussed for anomalous top-quark couplings in Ref. [2] as well as observables discussed for multi-Higgs models in Ref. [3]. Additional processes that have been discussed recently include W and Z pair production and decay [4]. On the other hand, CP conserving “naive- T ” odd triple-product correlations have been studied in radiative top-quark decay [5] at one-loop level.

In this paper we consider triple-product correlations in top-quark pair production at the LHC, induced by new CP violating interactions in a scalar sector extended with a color-octet electroweak-doublet as described in Ref. [6]. This model incorporates the additional scalars in a manner consistent with minimal flavor violation (MFV) in order to naturally suppress flavor changing neutral currents (FCNC).

Of particular interest to us are the two neutral, color-octet, scalar resonances that occur in the model, $S_{I,R}$. These particles couple at the one-loop level to two gluons and their production at the LHC has been discussed in Ref. [7] for the CP conserving case. These particles also couple (dominantly) to top-quark pairs which makes them an ideal candidate to study CP violation in the process $gg \rightarrow S_{I,R} \rightarrow t\bar{t}$. To this end, we extend the results of Ref. [7] to include CP violation, which can occur both in the couplings of $S_{I,R}$ to top-quark pairs as well as in certain self-interactions in the scalar potential. We further assume that top-quark decay proceeds as in the SM and serves only to analyze the corresponding spin. Within this framework we find that relatively large raw asymmetries are possible, as large as $\sim 12\%$. These raw asymmetries are diluted by the SM top-quark pairs and their observation is contingent on the resonance itself being observable. For illustration, we present a set of parameters for which the resonance is visible over the SM background and the resulting CP asymmetry can be as large as a few percent. We also comment on other channels where CP asymmetries are potentially visible in cases where the single resonance is not.

The LHC has already established new constraints on the new physics beyond the SM, even though it has been operating so far with a reduced energy of 7 TeV. In particular, both ATLAS and CMS have excluded certain color-octet scalars similar to the ones we consider here in a broad mass range [8] by studying the dijet channel. These exclusion limits, while interesting, do not apply to the models we discuss, where the color-octet resonances decay

almost exclusively into top-quark pairs. Their decay modes into dijets occur with branching ratios below 10^{-3} for the sets of parameters we use in this study.

Our paper is organized as follows: in Section II we review the relevant aspects of the model for the color-octet scalars with emphasis on the CP violating phases that have not been studied previously. In Section III we study several benchmark cases that illustrate the generic properties of the raw CP asymmetries. We also discuss several aspects concerning the observability of the CP violating signals at the LHC. In Section IV we state our conclusions and, finally, we relegate some analytic formulae to the Appendix.

II. COLOR-OCTET SCALARS AS A SOURCE FOR CP VIOLATION

We briefly review the case of a scalar sector that has been extended with a color-octet electroweak-doublet scalar with hypercharge $1/2$, $O = (8, 2, 1/2)$. This particular choice is motivated by the requirement of MFV and has been recently elaborated in Ref. [6, 7]. It was noted in these papers that in a MFV scenario only scalars with the same gauge quantum numbers as the SM Higgs doublet $H = (1, 2, 1/2)$ or color-octet scalars with the same weak quantum number as the Higgs doublet $O = (8, 2, 1/2)$ can couple to quarks, and this has many interesting consequences for both collider and flavor physics. This color-octet electroweak doublet can be written in the properly normalized component form with the color index A as $O = \sqrt{2}S = \sqrt{2} T^A(S^{A+}, S^{A0})^T$, where T^A is the $SU(3)_C$ generator normalized as $\text{Tr}(T^A T^B) = \delta^{AB}/2$.

The Yukawa couplings of the color-octet scalars can be parameterized, to the leading order, with the MFV assumption as [6]

$$\begin{aligned} \mathcal{L} = & -\frac{\sqrt{2}}{v}\tilde{\eta}_U\bar{U}_R T^A \hat{M}^u U_L S^{A0} + \frac{\sqrt{2}}{v}\tilde{\eta}_U\bar{U}_R T^A \hat{M}^u V_{KM} D_L S^{A+} \\ & - \frac{\sqrt{2}}{v}\tilde{\eta}_D\bar{D}_R T^A \hat{M}^d D_L S^{A0\dagger} - \frac{\sqrt{2}}{v}\tilde{\eta}_D\bar{D}_R T^A \hat{M}^u V_{KM}^\dagger U_L S^{A-} + h.c., \end{aligned} \quad (1)$$

where $\hat{M}^{u,d}$ are the diagonalized mass matrices, $\hat{M}^{u,d} = \text{diag}(m_{u,d}, m_{c,s}, m_{t,b})$; $U_{L,R}$ and $D_{L,R}$ are the up and down quarks, $U_{L,R} = \text{diag}(u_{L,R}, c_{L,R}, t_{L,R})$ and $D_{L,R} = \text{diag}(d_{L,R}, s_{L,R}, b_{L,R})$; and $v \sim 246$ GeV is the Higgs vacuum expectation value (VEV), $\langle H \rangle = v/\sqrt{2}$. The neutral complex field S^{A0} can be further decomposed into a scalar S_R^{A0} and a pseudo-scalar S_I^{A0} as $S^{A0} = (S_R^{A0} + iS_I^{A0})/\sqrt{2}$. The parameters $\tilde{\eta}_{U,D}$ are expected to be of order one and are in general complex. We will write them as $\tilde{\eta}_{U,D} = \eta_{U,D}e^{i\alpha_{u,d}}$ with $\eta_{U,D}$ real, and if there are non-zero phases $\alpha_{u,d}$ there is CP violation beyond the SM.

There is a second possible source of CP violation in this model in two of the self couplings appearing in the scalar potential. The most general potential with the complex scalar doublets H and S is given by [6],

$$\begin{aligned} V = & \frac{\lambda}{4} \left(H^\dagger H_i - \frac{v^2}{2} \right)^2 + 2m_s^2 \text{Tr} S^\dagger S_i + \lambda_1 H^\dagger H_i \text{Tr} S^{\dagger j} S_j + \lambda_2 H^\dagger H_j \text{Tr} S^{\dagger j} S_i \\ & + [\tilde{\lambda}_3 H^\dagger H^{\dagger j} \text{Tr} S_i S_j + \tilde{\lambda}_4 H^\dagger H^{\dagger i} \text{Tr} S^{\dagger j} S_j S_i + \tilde{\lambda}_5 H^\dagger H^{\dagger i} \text{Tr} S^{\dagger j} S_i S_j + h.c.] \\ & + \lambda_6 \text{Tr} S^\dagger S_i S^{\dagger j} S_j + \lambda_7 \text{Tr} S^\dagger S_j S^{\dagger j} S_i + \lambda_8 \text{Tr} S^\dagger S_i \text{Tr} S^{\dagger j} S_j \end{aligned}$$

$$+ \lambda_9 \text{Tr } S^{\dagger i} S_j \text{Tr } S^{\dagger j} S_i + \lambda_{10} \text{Tr } S_i S_j S^{\dagger i} S^{\dagger j} + \lambda_{11} \text{Tr } S_i S_j S^{\dagger j} S^{\dagger i} . \quad (2)$$

The parameters $\tilde{\lambda}_{3,4,5}$ are in general complex, but without loss of generality, one can choose a convention in which $\tilde{\lambda}_3 = \lambda_3$ is real. The two other phases cannot be removed and we write them as $\tilde{\lambda}_{4,5} = \lambda_{4,5} e^{i\alpha_{4,5}}$. Non-zero phases $\alpha_{4,5}$ provide the second source of CP violation beyond the SM present in the model. We note the custodial symmetry requires $\lambda_4 = \lambda_5^*$ [9, 10], so that $\alpha_4 = -\alpha_5$ in our parameterization.

If the mass of color-octet scalars is not too large, a tree-level interaction can pair produce them at the LHC through the process $gg \rightarrow S^\dagger S$. Since the color-octet scalars also couple to quarks, there is an additional contribution from $q\bar{q} \rightarrow S^\dagger S$. However this contribution is small because the Yukawa couplings of S to quarks are proportional to quark masses. Single S production is also possible at tree level from its Yukawa couplings to quarks, but this tree-level contribution is small as it is proportional to the light-quark mass. It has been shown that the single S production cross section at the LHC is dominated by a loop induced $gg - S$ interaction and can be of order 100 fb for masses of order a few hundred GeV to a TeV [7]. If these resonances are produced at the LHC, it will be possible to study their properties, including CP violation, through their decays to SM particles. The dominant decay mode is $S \rightarrow t\bar{t}$ although there is also one-loop induced decay into gluon pair: $S \rightarrow gg$ [6, 7].

In this paper we wish to study signals of CP violation at the LHC. This is accomplished by first observing the resonant production of the neutral color-octet scalars $S_{I,R}$ through their effective $gg - S$ couplings and then studying the correlations that occur in the subsequent decay chain: $gg \rightarrow S_{I,R} \rightarrow t\bar{t} \rightarrow b\bar{b}\mu^+\mu^-\nu\bar{\nu}$. The new sources of CP violation induce triple-product correlations involving the spin of the top and anti-top quarks which are subsequently analyzed by their weak decays. In the dimuon mode chosen above, it is the direction of the muons that analyzes the spin directions. Both the new sources of CP violation contribute to the resulting asymmetries.

The relevant effective couplings are shown schematically in Figure 1, and they can be written in terms of an effective Lagrangian as

$$\begin{aligned} \mathcal{L}(S - t\bar{t}) &= \bar{t}(a_R + ib_R\gamma_5)T^A t S_R^{A0} + \bar{t}(a_I + ib_I\gamma_5)T^A t S_I^{A0} , \\ \mathcal{L}(S - gg) &= (F_R^a G_{\mu\nu}^A G^{B\mu\nu} + F_R^b \tilde{G}_{\mu\nu}^A G^{B\mu\nu})d^{ABC} S_R^{A0} \\ &\quad + (F_I^a G_{\mu\nu}^A G^{B\mu\nu} + F_I^b \tilde{G}_{\mu\nu}^A G^{B\mu\nu})d^{ABC} S_I^{A0} , \end{aligned} \quad (3)$$

where $G_{\mu\nu}^A$ is the gluon field strength tensor and $\tilde{G}^{A\mu\nu} = (1/2)\epsilon^{\mu\nu\alpha\beta}G_{\alpha\beta}^A$.

The couplings to the top-quark occur at tree-level and they contain CP violation originating in the new phase $\tilde{\eta}_U$. They are given by

$$\begin{aligned} S_R^{A0} - t\bar{t} : \quad i(a_R + ib_R\gamma_5) &= -i\eta_U \frac{m_t}{v} (\cos \alpha_u - i \sin \alpha_u \gamma_5) T^A , \\ S_I^{A0} - t\bar{t} : \quad i(a_I + ib_I\gamma_5) &= i\eta_U \frac{m_t}{v} (\sin \alpha_u + i \cos \alpha_u \gamma_5) T^A . \end{aligned} \quad (4)$$

The couplings to gluons occur at one-loop level and can be easily derived following Ref. [7]. The CP violation in this case is due to phases in the couplings $\tilde{\lambda}_{4,5}$. We find

$$F_R^a = (\sqrt{2}G_F)^{1/2} \frac{\alpha_s}{8\pi} \left[\eta_U \cos \alpha_u I_q \left(\frac{m_t^2}{m_R^2} \right) \right]$$

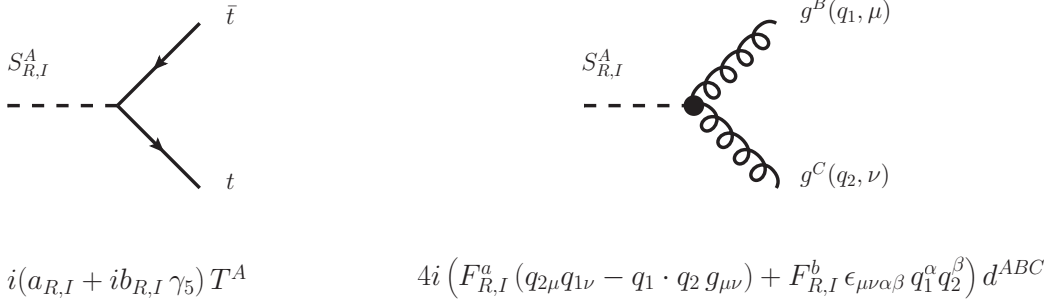


FIG. 1: Feynman Rules.

$$\begin{aligned}
& - \frac{9}{4} \frac{v^2}{m_R^2} (\lambda_4 \cos \alpha_4 + \lambda_5 \cos \alpha_5) \left\{ \frac{1}{2} I_s(1) + \frac{1}{2} I_s \left(\frac{m_I^2}{m_R^2} \right) \right\} \Bigg] , \\
F_R^b &= (\sqrt{2} G_F)^{1/2} \frac{\alpha_s}{8\pi} \frac{1}{2} \frac{m_t^2}{m_R^2} \eta_U \sin \alpha_u f \left(\frac{m_t^2}{m_R^2} \right) , \\
F_I^a &= (\sqrt{2} G_F)^{1/2} \frac{\alpha_s}{8\pi} \left[-\eta_U \sin \alpha_u I_q \left(\frac{m_t^2}{m_I^2} \right) \right. \\
& \quad \left. + \frac{9}{4} \frac{v^2}{m_I^2} (\lambda_4 \sin \alpha_4 + \lambda_5 \sin \alpha_5) \left\{ \frac{5}{6} I_s(1) + \frac{1}{6} I_s \left(\frac{m_R^2}{m_I^2} \right) \right\} \right] , \\
F_I^b &= (\sqrt{2} G_F)^{1/2} \frac{\alpha_s}{8\pi} \frac{1}{2} \frac{m_t^2}{m_I^2} \eta_U \cos \alpha_u f \left(\frac{m_t^2}{m_I^2} \right) . \tag{5}
\end{aligned}$$

In these expressions we have assumed that the mass of the charged color-octet scalars S^\pm is equal to the mass of S_I , $m^\pm = m_I$, which corresponds to the custodial symmetry conserving case where $2\lambda_3 = \lambda_2$ [6]. We have allowed for the mass of S_R to be different, $m_R \neq m_I$. These two masses are related by $m_R^2 - m_I^2 = \lambda_3 v^2$. Throughout the calculation, the scalars S_R and S_I (when not in a loop), are taken to be on-shell, in keeping with the narrow width approximation. The loop functions $I_{q,s}$ and f are defined by:

$$\begin{aligned}
I_q(z) &= 2z + z(4z - 1)f(z), \quad I_s(z) = -z(1 + 2zf(z)), \\
f(z) &= \frac{1}{2} \left(\ln \left(\frac{1 + \sqrt{1 - 4z}}{1 - \sqrt{1 - 4z}} \right) - i\pi \right)^2 \quad \text{for } z < 1/4 \\
&= -2 \left(\arcsin \left(\frac{1}{2\sqrt{z}} \right) \right)^2 \quad \text{for } z > 1/4. \tag{6}
\end{aligned}$$

From this it follows that $I_s(1) = \pi^2/9 - 1$, a factor that generates some suppression in contributions from scalar loops relative to top-quark loops.

III. ESTIMATE OF CP-ODD ASYMMETRIES

We will now give numerical estimates for the triple-product correlations that will serve as CP -odd observables. Following Ref. [2], we know that the best observable for the case of

$t\bar{t}$ production and decay is the correlation

$$\tilde{\mathcal{O}}_1 = \epsilon_{\mu\nu\alpha\beta} p_b^\mu p_{\bar{b}}^\nu p_{\mu^+}^\alpha p_{\mu^-}^\beta \xrightarrow{b\bar{b} \text{ CM}} \propto \vec{p}_b \cdot (\vec{p}_{\mu^+} \times \vec{p}_{\mu^-}). \quad (7)$$

The first, covariant, expression is given in terms of the completely antisymmetric Levi-Civita tensor, whereas the second one indicates its reduction to a simple triple-product correlation in the $b\bar{b}$ center-of-mass frame. The reasons to select this correlation from the set described in Ref. [2] are twofold. First, the dimuon decay of $t\bar{t}$ is the cleanest. Second, the fact that the $t\bar{t}$ pair is produced from a scalar intermediate state prevents the appearance of correlations involving the beam momentum. Note that although it appears that this correlation requires distinguishing the b and \bar{b} jets, it is only necessary to systematically associate one of the b jets with one of the muons. For example, the " b "-jet could be the one closest to the μ^+ .

To study the effect of the correlation Eq. (7) we consider the laboratory frame distribution $d\sigma/d\tilde{\mathcal{O}}_1$. The CP violating effects can be isolated by extracting asymmetric terms from this distribution, either by a direct fit or by constructing the integrated counting asymmetry

$$A_1 \equiv \frac{N_{events}(\tilde{\mathcal{O}}_1 > 0) - N_{events}(\tilde{\mathcal{O}}_1 < 0)}{N_{events}(\tilde{\mathcal{O}}_1 > 0) + N_{events}(\tilde{\mathcal{O}}_1 < 0)}. \quad (8)$$

To measure this distribution (and its associated integrated asymmetry) we generate events for the process $pp \rightarrow S_{I,R} \rightarrow t\bar{t} \rightarrow b\mu^+\nu_\mu\bar{b}\mu^-\bar{\nu}_\mu$ with the aid of **MadGraph** [11]. To generate the signal events we implement the vertices of Figure 1 into the **MadGraph** code. We also use the default **MadGraph** SM processes to generate the corresponding events. In all cases we use the default **MadGraph** cuts requiring the top quark and W boson intermediate states to be within 15 widths of their mass shell, the transverse momentum p_T of both muons to be larger than 10 GeV and the pseudo-rapidity of both muons to be $|\eta_\mu| < 2.5$. We also use SM parameter values as in **MadGraph** and the CTEQ-6L1 parton distribution functions [12].

We begin by presenting raw asymmetries (no SM top-quark pair events) using values for the parameters η_U and $\lambda_{4,5}$ in the ranges discussed in Ref. [7], as well as $m_{I,R} \lesssim 1$ TeV. We illustrate the CP asymmetries utilizing only the dimuon signal, but emphasize that other decay modes can also be used.

The results are summarized in Table I where we show for each set of parameters the corresponding resonance ($S_{I,R}$) widths (which are completely dominated by the $t\bar{t}$ decay mode); production cross-sections at the LHC $\sigma(pp \rightarrow S_{I,R} \rightarrow t\bar{t} \rightarrow b\bar{b}\mu^+\mu^-\nu\bar{\nu})$ for $\sqrt{S} = 14$ TeV; and a raw asymmetry. This raw asymmetry is estimated separately for each resonance by including only top-quark pair events that result from the decay of that resonance and have an invariant mass within 10 GeV of the resonance, $|m_{t\bar{t}} - m_{I,R}| < 10$ GeV.

We begin with Case 1 in which we have two well separated resonances, $m_R = 500$ GeV and $m_I = 700$ GeV, $|m_R - m_I| \gg \Gamma_{I,R}$. The scalar potential parameters $\lambda_{4,5}$, as well as the parameter η_U governing the strength of the $S t\bar{t}$ coupling, are all chosen to be one for illustration. We also choose CP violating phases to be $\alpha_u = \pi/4$, $\alpha_{4,5} = 0$, in order to maximize the CP violating interaction in the coupling of scalars to $t\bar{t}$. As seen in Table I, the resulting raw asymmetry can be rather large, about 12% for each resonance. The results

	Parameters	Decay Width [GeV]	Resonance cross-section [fb]	Raw asymmetry around resonance
Case 1	$m_R, m_I = 500, 700 \text{ GeV},$ $\eta_U = \lambda_{4,5} = 1, \alpha_u = \pi/4$	$S_R : 2.7$ $S_I : 5.3$	$S_R : 5.9$ $S_I : 2.8$	$S_R : A_1 = -0.123$ $S_I : A_1 = 0.121$
Case 2	$m_R, m_I = 500, 700 \text{ GeV},$ $\eta_U = 1, \lambda_{4,5} = 8, \alpha_{u,4} = -\alpha_5 = \pi/4$	$S_R : 2.7$ $S_I : 5.3$	$S_R : 6.5$ $S_I : 2.8$	$S_R : A_1 = -0.125$ $S_I : A_1 = 0.123$
Case 3	$m_R, m_I = 500, 700 \text{ GeV},$ $\eta_U = \lambda_{4,5} = 1, \alpha_u = \pi/8$	$S_R : 2.1$ $S_I : 5.8$	$S_R : 7.2$ $S_I : 3.1$	$S_R : A_1 = -0.112$ $S_I : A_1 = 0.084$
Case 4	$m_R = m_I = 500 \text{ GeV},$ $\eta_U = \lambda_{4,5} = 1, \alpha_u = \pi/8$	$S_R : 2.1$ $S_I : 3.3$	$S_R + S_I : 12.3$	$S_R + S_I : A_1 = -0.017$
Case 5	$m_R, m_I = 400, 1000 \text{ GeV},$ $\eta_U = \lambda_{4,5} = 1, \alpha_u = \pi/4$	$S_R : 1.2$ $S_I : 8.8$	$S_R : 8.9$ $S_I : 1.1$	$S_R : A_1 = -0.089$ $S_I : A_1 = 0.096$

TABLE I: Parameter values, resonance $S_{I,R}$ decay-widths and production cross-sections $\sigma(pp \rightarrow S_{I,R} \rightarrow t\bar{t} \rightarrow b\bar{b}\mu^+\mu^-\nu\bar{\nu})$ at the LHC $\sqrt{S} = 14 \text{ TeV}$, and raw CP asymmetry for the five cases discussed in the text. The raw asymmetry is defined by taking into account the events with $|m_{t\bar{t}} - m_{I,R}| < 10 \text{ GeV}$.

also show that the two resonances produce asymmetries that tend to cancel each other out, as can be inferred from Eq. (B3). In Fig. 2, we plot the $d\sigma/d\tilde{\mathcal{O}}_1$ distributions for the two scalars, where $\tilde{\mathcal{O}}_1$ is evaluated as $\tilde{\mathcal{O}}_1 = \vec{p}_b \cdot (\vec{p}_{\mu^+} \times \vec{p}_{\mu^-})/m_t^3$ in the $b\bar{b}$ rest-frame. The solid and dot-dashed lines show the CP violating case whereas the thin dashed lines illustrate the corresponding CP conserving case where the phases have been set to zero.

In Case 2 we choose much larger values for the parameters $\lambda_{4,5}$, taking them to be 8 times larger than η_U . With this choice we want to enhance the relative contribution from the scalar loops which are otherwise suppressed by the factor $(\pi^2/9 - 1)$ mentioned before. We also introduce non-zero CP phases $\alpha_{4,5}$. We find that this choice produces a modest increase in the cross-section for S_R but not for S_I . The raw CP asymmetries remain about the same indicating that the top quark loop is still dominant.

In Case 3 we repeat the parameters of Case 1 except for choosing $\alpha_U = \pi/8$ which has the effect of minimizing the cancellation of asymmetries between the two resonances. This can be seen from the Table I where the asymmetry around S_R remains near 12% but the asymmetry near S_I is down to about 8%. The production cross-section for each resonance is also larger with this choice of phase and the widths are affected as well with S_R becoming narrower and S_I wider.

As Eq. (B4) indicates, when the two masses $m_{I,R}$ are close to each other, the contribution from the top-quark loop tends to cancel out, exposing the effect of $\lambda_{4,5}$. We illustrate this in Case 4 with $m_I = m_R$ and CP phase $\alpha_u = \pi/8$. The resulting raw asymmetry is smaller but non-vanishing.

Finally, in Case 5, we illustrate the effect of the resonance mass by choosing one of the

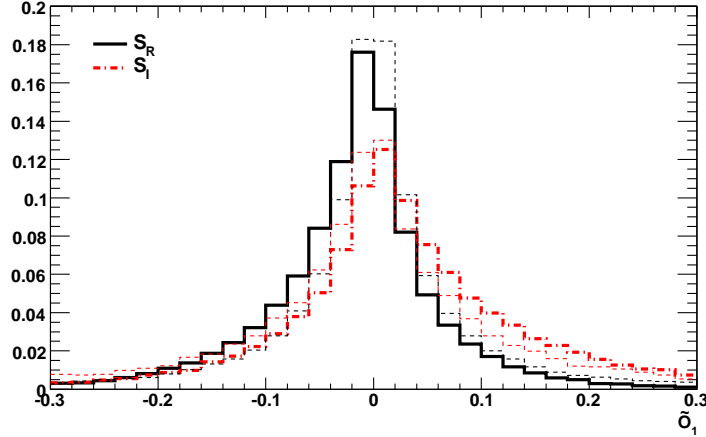


FIG. 2: $d\sigma/d\tilde{O}_1$ distributions for the events with $|m_{t\bar{t}} - m_{R,I}| < 10$ GeV in Case 1, where the SM contribution is omitted. Thin dashed lines are for the zero CP phase case, but the same masses and couplings as in Case 1.

resonances to be just above the $t\bar{t}$ threshold and the other one near the high-end of the LHC reach. With the same CP phases as in Case 1, the asymmetries are about 25% smaller in this case.

We now turn to the question of observability of the raw asymmetries over the SM background of top-quark pairs. First, there is a matter of statistical sensitivity. At the LHC, the total cross-section for $t\bar{t}$ events is approximately $\sigma_{t\bar{t}} = 850$ pb. This implies that the expected number of events in the dimuon channel is about 10^5 for an integrated luminosity $\mathcal{L} = 10$ [fb $^{-1}$]. Therefore, an optimistic sensitivity for the asymmetry *using only the dimuon channel* for one year of nominal LHC running, is $\delta A_1 = 1/\sqrt{\sigma_{t\bar{t}} * B_{\mu\mu} * \mathcal{L}} \sim 3 \times 10^{-3}$, where $B_{\mu\mu} \simeq 1/81$ is the branching ratio of the dimuon channel. Of course this can be improved significantly by considering other decay channels. For example, in Ref. [2] it is shown how to use the lepton-plus-jets channel and purely hadronic channels to measure CP asymmetries. A detailed analysis of all channels is beyond the scope of the present paper where we simply seek to establish the possibility of a large raw asymmetry.

Second, as we have seen, the asymmetries due to the two resonances tend to cancel. This indicates the need to isolate a certain window in top-quark pair invariant mass around the resonance to extract a non-zero asymmetry. In the dimuon channel it is not possible to reconstruct $m_{t\bar{t}}$ so we use the transverse mass M_T for this purpose.¹ The correlation between these two variables is shown in Figure 3.

This complication would also be treated differently in other top-quark decay channels,

¹ The transverse mass M_T is defined as $M_T = \sqrt{(\cancel{E}_T + E_T^{\ell\ell} + E_T^{b\bar{b}})^2 - (\vec{p}_T + \vec{p}_T^{\ell\ell} + \vec{p}_T^{b\bar{b}})^2}$, where $\cancel{E}_T = |\vec{p}_T|$, \vec{p}_T is missing transverse momentum, $\vec{p}_T^{\ell\ell(b\bar{b})}$ is vector-sum of dimuon ($b\bar{b}$ pair) transverse momentum, $E_T^{\ell\ell(b\bar{b})} = \sqrt{m_{\ell\ell(b\bar{b})}^2 + |\vec{p}_T^{\ell\ell(b\bar{b})}|^2}$ with $m_{\ell\ell(b\bar{b})}$ the invariant-mass of dimuon ($b\bar{b}$ pair).

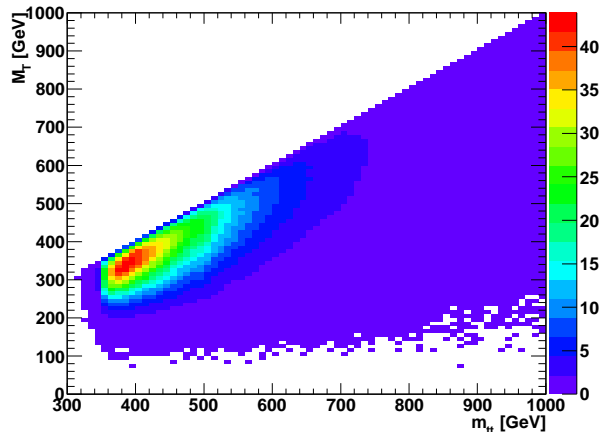


FIG. 3: Two-dimensional density plot of $m_{t\bar{t}}$ and M_T , for the $t\bar{t}$ production in the dimuon mode.

and its resolution will ultimately depend on an observation of a new resonance in $t\bar{t}$ events. At the same time, it shows that if one wants to check for CP asymmetries in $t\bar{t}$ events in which a resonance has not been observed, there are good reasons to study separately different small windows in $m_{t\bar{t}}$ (or the corresponding observable such as M_T), as small as allowed by statistics.

The resonant cross-section for all the cases discussed in Table I is significantly smaller than the cross-section for SM top-quark pairs in a 20 GeV window in $m_{t\bar{t}}$ which is ~ 280 fb when the window is centered at $m_{t\bar{t}} = 500$ GeV. This number is valid at leading order, including branching ratios for decay into dimuon channel, and including all the kinematic cuts discussed before. The SM events will thus dilute the raw asymmetries by two orders of magnitude making them unobservable for practical purposes. In other words, the large raw asymmetries in Table I are not observable at the LHC because the corresponding resonances do not stand out above the SM background. To continue our discussion we thus consider resonances with larger production cross-section. This can be easily achieved by increasing $\eta_U = 1$ to $\eta_U = 3$, which results in an order of magnitude increase in the resonance cross-sections without changing the asymmetries significantly.² We illustrate this in Table II. Notice that we have kept the definition of the raw asymmetry with a 20 GeV window around the resonance as in Table I. This window does not cover a full width in all cases with $\eta_U = 3$, resulting in fractionally smaller asymmetries than would be possible. The precise optimization of the window size, although eventually important for measurement, is beyond the scope of this study. We now have examples of large raw asymmetries in resonances that may be observable over the SM background as can be seen in Figure 4.

In Table III we examine the CP asymmetries that result when all $t\bar{t}$ events are included

² The value of $\eta_U = 3$ in conjunction with masses below one TeV is slightly outside the parameter space allowed by R_b studied in Ref. [7]. We use it anyway as a simple way to illustrate a resonance that stands above SM background taking into consideration the imprecise nature of indirect constraints on new physics.

	Parameters	Decay Width [GeV]	Resonance cross-section [fb]	Raw asymmetry around resonance
Case 1'	$m_R, m_I = 500, 700 \text{ GeV},$ $\eta_U = 3, \lambda_{4,5} = 1, \alpha_u = \pi/4$	$S_R : 24.3$ $S_I : 47.7$	$S_R : 60.4$ $S_I : 24.0$	$S_R : A_1 = -0.127$ $S_I : A_1 = 0.103$
Case 2'	$m_R, m_I = 500, 700 \text{ GeV},$ $\eta_U = 3, \lambda_{4,5} = 8, \alpha_{u,4} = -\alpha_5 = \pi/4$	$S_R : 24.3$ $S_I : 47.7$	$S_R : 43.2$ $S_I : 24.2$	$S_R : A_1 = -0.122$ $S_I : A_1 = 0.129$
Case 3'	$m_R, m_I = 500, 700 \text{ GeV},$ $\eta_U = 3, \lambda_{4,5} = 1, \alpha_u = \pi/8$	$S_R : 18.8$ $S_I : 52.5$	$S_R : 75.8$ $S_I : 26.9$	$S_R : A_1 = -0.117$ $S_I : A_1 = 0.076$
Case 4'	$m_R = m_I = 500 \text{ GeV},$ $\eta_U = 3, \lambda_{4,5} = 1, \alpha_u = \pi/8$	$S_R : 18.8$ $S_I : 29.9$	$S_R + S_I : 118.2$	$S_R + S_I : A_1 = -0.029$
Case 5'	$m_R, m_I = 400, 1000 \text{ GeV},$ $\eta_U = 3, \lambda_{4,5} = 1, \alpha_u = \pi/4$	$S_R : 10.9$ $S_I : 79.0$	$S_R : 99.2$ $S_I : 9.1$	$S_R : A_1 = -0.089$ $S_I : A_1 = 0.082$

TABLE II: Parameter values, resonance $S_{I,R}$ decay-widths and production cross-sections $\sigma(pp \rightarrow S_{I,R} \rightarrow t\bar{t} \rightarrow b\bar{b}\mu^+\mu^-\nu\bar{\nu})$ at the LHC $\sqrt{S} = 14 \text{ TeV}$, and raw CP asymmetry for the five cases discussed in the text with $\eta_U = 3$. The raw asymmetry is defined by taking into account the events with $|m_{t\bar{t}} - m_{I,R}| < 10 \text{ GeV}$.

(SM plus new resonances). In the first column we show the asymmetry diluted by SM events. We define this asymmetry using a 20 GeV $m_{t\bar{t}}$ window around the resonance. As expected, it is roughly one order of magnitude smaller than the raw asymmetries for the resonant cross-sections shown in Table II, and larger for S_I which has a larger production cross-section. In the second column we show how the asymmetry becomes even smaller when the whole $m_{t\bar{t}}$ range is used, due to the partial cancellation between the two resonances. Finally, in the last column, we impose a realistic kinematic cut to simulate selecting different $m_{t\bar{t}}$ windows to separate the two scalar contributions. Note that the numbers in parenthesis in Table III give the statistical error in our simulation, which is expected to be the same order as the statistical error for $\mathcal{L} = 400 \text{ [fb}^{-1}\text{]}$ at the LHC.

IV. RESULTS AND CONCLUSION

We have investigated the CP violating asymmetries that result in $t\bar{t}$ events at the LHC from new sources of CP violation associated with color-octet scalars. We have considered the effect of two new sources of CP violation: a phase in the couplings of the new resonances $S_{I,R}$ to top-quarks; and two phases in the quartic couplings of the scalar potential. We find that the former is responsible for much larger CP violating effects than the latter. We have shown that these models typically induce large raw asymmetries that can reach 12%.

Observation of the asymmetries is contingent to observation of the new resonance itself and we have presented a rough numerical simulation that illustrates this. An optimistic

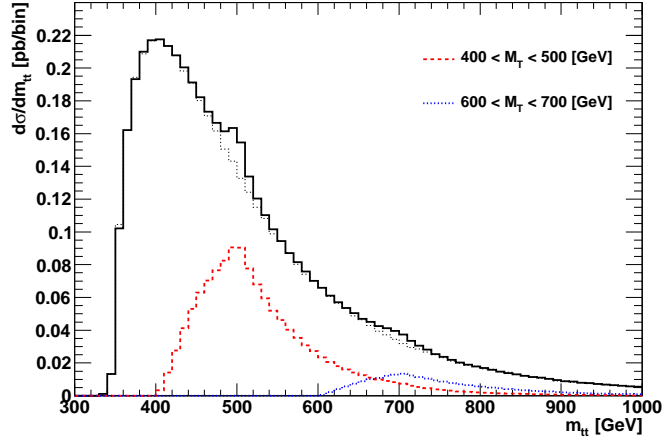


FIG. 4: $d\sigma/dm_{t\bar{t}}$ distributions without and with contribution of scalars in Case 1', plotted in dotted and solid line, respectively, in an unit of pb per 5 GeV bin. Dashed lines are for the distribution after $400 < M_T < 500$ [GeV] (red long-dashed) and $600 < M_T < 700$ [GeV] (blue short-dashed) cuts.

sensitivity for the asymmetry *using only the dimuon channel* could be $\delta A_1 \sim 3 \times 10^{-3}$ at the LHC with an integrated luminosity of $\mathcal{L} = 10$ [fb $^{-1}$], when the events in full kinematical region are taken into account. In Table III we have shown several examples utilizing kinematical cuts with resulting asymmetries enhanced as large as a few percent by enhancing the scalar resonance contribution and avoiding cancellation between the two scalar contributions, which could be observed at the LHC.

We have presented our analysis for the dimuon channel as this is the cleanest one. However, our study can be easily extended to other top-quark decay channels to increase statistics. We have studied the CP asymmetries only in the top-quark pair production channel via one new resonance. Other channels, such as SS pair production, also exhibit CP violating asymmetries and may be preferable in scenarios where the SS production cross-section exceeds the single S production cross-section.

Acknowledgments

This work was partially supported by NSC, NCTS, SJTU 985 grant, and Excellent Research Projects of National Taiwan University (NTU-98R0526), and in part by DOE under contract number DE-FG02-01ER41155. G.V. thanks the National Taiwan University, Taipei, Taiwan for their hospitality.

	Asymmetry around resonance including SM amplitudes	Integrated asymmetry including SM amplitudes	M_T cut
Case 1'	$S_R : A_1 = -0.017(2)$ $S_I : A_1 = 0.029(4)$	$A_1 = 0.0002(5)$	Low : $A_1 = -0.0045(10)$ High : $A_1 = 0.0141(23)$
Case 2'	$S_R : A_1 = -0.013(2)$ $S_I : A_1 = 0.021(4)$	$A_1 = -0.0007(5)$	Low : $A_1 = -0.0026(10)$ High : $A_1 = 0.0120(23)$
Case 3'	$S_R : A_1 = -0.026(2)$ $S_I : A_1 = 0.030(4)$	$A_1 = -0.0022(5)$	Low : $A_1 = -0.0071(10)$ High : $A_1 = 0.0136(23)$
Case 4'	$S_R + S_I :$ $A_1 = -0.009(2)$	$A_1 = -0.0003(5)$	Low : $A_1 = -0.0023(10)$
Case 5'	$S_R : A_1 = -0.021(2)$ $S_I : A_1 = 0.041(10)$	$A_1 = -0.0016(5)$	Low : $A_1 = -0.0059(8)$ High : $A_1 = 0.023(4)$

TABLE III: CP asymmetries for the illustrative cases of Table II including SM top-quark pair events. In the first column we define the asymmetry in the window $|m_{t\bar{t}} - m_{I,R}| < 10$ GeV. In the middle column, we show the integrated asymmetry over the full $m_{t\bar{t}}$ range. In the last column, we illustrate how to isolate the resonances with more realistic cuts in the transverse mass. We use $400 < M_T < 500$ [GeV] for low mass and $600 < M_T < 700$ [GeV] for high mass cuts for Cases 1' to 4'. For Case 5' we use $300 < M_T < 400$ [GeV] for low mass and $800 < M_T < 1000$ [GeV] for high mass cuts. The numbers in parenthesis are the statistical error in our simulation, which is expected to be the same order as the statistical error for $\mathcal{L} = 400$ [fb $^{-1}$] at the LHC.

Appendix A: CP Violation with a Higgs boson

We review the salient features of CP violation in $t\bar{t}$ production at the LHC induced by a new Higgs-boson as discussed in Ref. [3]. The CP violation in a suitable extended Higgs sector manifests itself in the form of a neutral Higgs mass eigenstate that has both scalar and pseudo-scalar couplings to the top-quark. In general these couplings can be written as

$$\mathcal{L} = -\frac{m_t}{v} H \bar{t} (A + iB\gamma_5) t, \quad (\text{A1})$$

where A, B are real and $A = 1, B = 0$ corresponds to the standard model with one Higgs doublet. Multi-Higgs models achieve maximal CP violation when $A = B$, and these couplings reach the Weinberg unitarity bound, $|AB| \lesssim \frac{1}{\sqrt{2}}$ [13].

This Higgs-boson is produced at the LHC mostly via gluon fusion. Both the scalar and pseudoscalar cases have been considered in the literature before and these results at leading order can be summarized by the effective couplings

$$\mathcal{L} = \left[F_a G_{\mu\nu} G^{\mu\nu} + F_b \tilde{G}_{\mu\nu} G^{\mu\nu} \right] H \quad (\text{A2})$$

The two form factors $F_a(s)$ and $F_b(s)$ can be found, for example in Ref. [14]. For the kinematic regime in which the Higgs boson is heavier than a $t\bar{t}$ pair they are given by

$$\begin{aligned} F_a &= \left(\sqrt{2}G_F\right)^{1/2} A \frac{\alpha_s}{12\pi} 3I_q(z) \\ F_b &= -\left(\sqrt{2}G_F\right)^{1/2} B \frac{\alpha_s}{8\pi} z f(z) \end{aligned} \quad (\text{A3})$$

with $z = m_t^2/m_H^2$, the functions $I_q(z)$ and $f(z)$ arise from the one-loop contribution of a top-quark loop and were given in Eq. (6).

The origin of the correlation, Eq. (7) in this model is a CP violating term in the invariant matrix element squared for $gg \rightarrow t\bar{t} \rightarrow b\bar{b}\mu^+\mu^-\nu\bar{\nu}$ of the form

$$|\mathcal{M}|^2 = C_1(s, t, u) \epsilon(p_t, p_{\bar{t}}, p_{\mu^+}, p_{\mu^-}) + \dots \quad (\text{A4})$$

The function $C_1(s, t, u)$ can be written in a compact form reflecting two contributions: the s channel Higgs amplitude squared; and the interference between the t and u channels ($gg \rightarrow t\bar{t}$ in a color singlet state) and the s -channel Higgs amplitude. They are given by

$$\begin{aligned} C_1(s, t, u) &= 24 K_{\ell\ell} AB(|F_a|^2 + |F_b|^2) \frac{s^2}{(s - m_H^2)^2 + m_H^2 \Gamma_H^2} \frac{m_t^4}{v^2} \\ &+ 8g_s^2 K_{\ell\ell} (B\text{Re}(F_a) + A\text{Re}(F_b)) \frac{s^2(s - m_H^2)}{((s - m_H^2)^2 + m_H^2 \Gamma_H^2)(s^2 - (t - u)^2)} \frac{m_t^4}{v}. \\ K_{\ell\ell} &\equiv g^8 (p_b \cdot p_\nu) (p_{\bar{b}} \cdot p_{\bar{\nu}}) \left(\frac{\pi}{m_t \Gamma_t}\right)^2 \left(\frac{\pi}{M_W \Gamma_W}\right)^2 \\ &\times \delta(p_t^2 - m_t^2) \delta(p_{\bar{t}}^2 - m_t^2) \delta(p_{W^+}^2 - M_W^2) \delta(p_{W^-}^2 - M_W^2). \end{aligned} \quad (\text{A5})$$

The delta functions in this expression reflect the use of the narrow-width approximation for all top-quark and W -boson propagators. If the Higgs boson is also narrow, the expression simplifies further to

$$C_1(s, t, u) = 24 K_{\ell\ell} AB(|F_a|^2 + |F_b|^2) \frac{s^2 m_t^4}{v^2} \left(\frac{\pi}{m_H \Gamma_H}\right) \delta(s - m_H^2) \quad (\text{A6})$$

Appendix B: CP Violation with color-octet scalars

In the color-octet model discussed in this paper, the CP violation in the process $gg \rightarrow t\bar{t} \rightarrow b\bar{b}\mu^+\mu^-\nu\bar{\nu}$ takes the same form as Eq. (A4) with the form factor of Eq. (A6) replaced by the sum of the contributions from the octet neutral scalars S_R and S_I . The overall color factor changes from 24 to 20/3, and in the narrow width approximation we have

$$\begin{aligned} C_1(s, t, u) &= \frac{20K_{\ell\ell}}{3} s^2 m_t^2 \left(a_R b_R (|F_R^a|^2 + |F_R^b|^2) \left(\frac{\pi}{m_R \Gamma_R}\right) \delta(s - m_R^2) \right. \\ &+ \left. a_I b_I (|F_I^a|^2 + |F_I^b|^2) \left(\frac{\pi}{m_I \Gamma_I}\right) \delta(s - m_I^2) \right) \end{aligned}$$

$$= \frac{20K_{\ell\ell}}{3} \frac{s^2 m_t^4}{v^2} \frac{\eta_U^2 s_u c_u}{16} \left(\left(\frac{\pi D_R}{m_R \Gamma_R} \right) \delta(s - m_R^2) + \left(\frac{\pi D_I}{m_I \Gamma_I} \right) \delta(s - m_I^2) \right). \quad (\text{B1})$$

Where we have introduced for compactness the notation, $s_i \equiv \sin \alpha_i$, $c_i \equiv \cos \alpha_i$. The coefficients $D_{I,R}$ can be written as

$$\begin{aligned} D_I &= 4\eta_U^2 \left\{ c_u^2 + s_u^2 \left(1 - \frac{4m_t^2}{m_I^2} \right)^2 \right\} \frac{m_t^4}{m_I^4} \left| f \left(\frac{m_t^2}{m_I^2} \right) \right|^2 \\ &\quad - 72\eta_U s_u (\lambda_4 s_4 + \lambda_5 s_5) \text{Re} \left\{ \left[\frac{5}{6} I_s(1) + \frac{1}{6} I_s \left(\frac{m_R^2}{m_I^2} \right) \right] I_q^* \left(\frac{m_t^2}{m_I^2} \right) \right\} \\ &\quad + 81 (\lambda_4 s_4 + \lambda_5 s_5)^2 \left| \frac{5}{6} I_s(1) + \frac{1}{6} I_s \left(\frac{m_R^2}{m_I^2} \right) \right|^2 \end{aligned} \quad (\text{B2})$$

$$\begin{aligned} D_R &= -4\eta_U^2 \left\{ s_u^2 + c_u^2 \left(1 - \frac{4m_t^2}{m_R^2} \right)^2 \right\} \frac{m_t^4}{m_R^4} \left| f \left(\frac{m_t^2}{m_R^2} \right) \right|^2 \\ &\quad + 72\eta_U c_u (\lambda_4 c_4 + \lambda_5 c_5) \text{Re} \left\{ \left[\frac{1}{2} I_s(1) + \frac{1}{2} I_s \left(\frac{m_I^2}{m_R^2} \right) \right] I_q^* \left(\frac{m_t^2}{m_R^2} \right) \right\} \\ &\quad - 81 (\lambda_4 c_4 + \lambda_5 c_5)^2 \left| \frac{1}{2} I_s(1) + \frac{1}{2} I_s \left(\frac{m_I^2}{m_R^2} \right) \right|^2 \end{aligned} \quad (\text{B3})$$

If the two neutral scalars have masses that are close to each other (recall that $m_R^2 - m_I^2 = \lambda_3 v^2$) then the form factor becomes

$$\begin{aligned} C_1(s, t, u) &= \frac{20K_{\ell\ell}}{3} s^2 m_t^2 \left[\frac{a_R b_R (|F_R^a|^2 + |F_R^b|^2)}{(s - m_R^2)^2 + m_R^2 \Gamma_R^2} + \frac{a_I b_I (|F_I^a|^2 + |F_I^b|^2)}{(s - m_I^2)^2 + m_I^2 \Gamma_I^2} \right. \\ &\quad \left. + (s - m_R^2)(s - m_I^2) \frac{\text{Re}(a_R b_I (F_R^a F_I^{a*} + F_R^b F_I^{b*}) + a_I b_R (F_R^{a*} F_I^a + F_R^{b*} F_I^b))}{2((s - m_I^2)^2 + m_I^2 \Gamma_I^2)((s - m_R^2)^2 + m_R^2 \Gamma_R^2)} \right] \\ &\quad + \frac{20g_s^2 K_{\ell\ell}}{3} \frac{s^2 m_t^4}{v(s^2 - (t - u)^2)} \left[\frac{(b_R \text{Re}(F_R^a) + a_R \text{Re}(F_R^b)) (s - m_R^2)}{((s - m_R^2)^2 + m_R^2 \Gamma_R^2)} \right. \\ &\quad \left. + \frac{(b_I \text{Re}(F_I^a) + a_I \text{Re}(F_I^b)) (s - m_I^2)}{((s - m_I^2)^2 + m_I^2 \Gamma_I^2)} \right] \\ &= \frac{20K_{\ell\ell}}{3} \frac{s^2 m_t^4}{16v^2} \frac{\eta_U^2}{(s - m_S^2)^2 + m_S^2 \Gamma_S^2} 9 (\lambda_4 \sin(\alpha_4 - \alpha_u) + \lambda_5 \sin(\alpha_5 - \alpha_u)) \\ &\quad \times (-4\eta_U I_s(1) \text{Re}(I_q(m_t^2/m_S^2)) + 9I_s^2(1) (\lambda_4 \cos(\alpha_4 - \alpha_u) + \lambda_5 \cos(\alpha_5 - \alpha_u))) \\ &\quad + \mathcal{O}(m_R - m_I) \end{aligned} \quad (\text{B4})$$

where in the last line we have used $m_S \simeq m_R \simeq m_I$ and similarly for Γ_S . The first two terms correspond to those in Eq. (B1) without the narrow width approximation for $S_{I,R}$, and the third term arises from the interference between the two resonances. Next, we have also kept the term arising from the interference of the scalar exchange amplitude and the QCD background, analogous to the second term in Eq. (A5). For the color-octet case, the overall color factor in this term changes from 4 to 10/3 and the interference still occurs only

with the t and u channels of the QCD amplitude. The s -channel gluon exchange diagram has a color structure that does not interfere with the color-octet scalar exchange amplitudes. As can be seen from the second expression, the two resonances tend to cancel each other out. For degenerate resonances only a small term proportional to the scalar loops remains. The corrections to this limit, proportional to $(m_R - m_I)$ are too cumbersome to write out explicitly and are best studied numerically.

Appendix C: Decay width of $S_{I,R}$

Dominant decay mode of $S_{I,R}$ is $t\bar{t}$ mode. The partial decay width is given as follows [6];

$$\Gamma(S_R \rightarrow t\bar{t}) = \frac{m_R \eta_U^2 m_t^2}{16\pi v^2} \sqrt{1 - \frac{4m_t^2}{m_R^2}} \left[1 - \frac{4m_t^2}{m_R^2} c_u^2 \right], \quad (C1)$$

$$\Gamma(S_I \rightarrow t\bar{t}) = \frac{m_I \eta_U^2 m_t^2}{16\pi v^2} \sqrt{1 - \frac{4m_t^2}{m_I^2}} \left[1 - \frac{4m_t^2}{m_I^2} s_u^2 \right]. \quad (C2)$$

The partial decay width into gg , which is related to the production cross-section, is give as follows;

$$\begin{aligned} \Gamma(S_R \rightarrow gg) = & \frac{G_F m_R^3 C_1 \alpha_S^2}{\sqrt{2} 2^{10} \pi^3} \left[\eta_U^2 c_u^2 \left| I_q \left(\frac{m_t^2}{m_R^2} \right) \right|^2 \right. \\ & - \frac{9}{2} \frac{v^2}{m_R^2} \eta_U c_u (\lambda_4 c_4 + \lambda_5 c_5) \operatorname{Re} \left\{ \left[\frac{1}{2} I_s(1) + \frac{1}{2} I_s \left(\frac{m_I^2}{m_R^2} \right) \right] I_q^* \left(\frac{m_t^2}{m_R^2} \right) \right\} \\ & \left. + \frac{81}{16} \frac{v^4}{m_R^4} (\lambda_4 c_4 + \lambda_5 c_5)^2 \left| \frac{1}{2} I_s(1) + \frac{1}{2} I_s \left(\frac{m_I^2}{m_R^2} \right) \right|^2 + \eta_U^2 s_u^2 \frac{m_t^4}{m_R^4} \left| f \left(\frac{m_t^2}{m_R^2} \right) \right|^2 \right], \end{aligned} \quad (C3)$$

$$\begin{aligned} \Gamma(S_I \rightarrow gg) = & \frac{G_F m_I^3 C_1 \alpha_S^2}{\sqrt{2} 2^{10} \pi^3} \left[\eta_U^2 s_u^2 \left| I_q \left(\frac{m_t^2}{m_I^2} \right) \right|^2 \right. \\ & - \frac{9}{2} \frac{v^2}{m_I^2} \eta_U s_u (\lambda_4 s_4 + \lambda_5 s_5) \operatorname{Re} \left\{ \left[\frac{5}{6} I_s(1) + \frac{1}{6} I_s \left(\frac{m_R^2}{m_I^2} \right) \right] I_q^* \left(\frac{m_t^2}{m_I^2} \right) \right\} \\ & \left. + \frac{81}{16} \frac{v^4}{m_I^4} (\lambda_4 s_4 + \lambda_5 s_5)^2 \left| \frac{5}{6} I_s(1) + \frac{1}{6} I_s \left(\frac{m_R^2}{m_I^2} \right) \right|^2 + \eta_U^2 c_u^2 \frac{m_t^4}{m_I^4} \left| f \left(\frac{m_t^2}{m_I^2} \right) \right|^2 \right], \end{aligned} \quad (C4)$$

where a color-factor $C_1 = 40/3$. In the $\alpha_{u,4,5} \rightarrow 0$ limit, Eq. (C3) and (C4) coincide with Eq. (25) and (29) of Ref. [7], respectively.

-
- [1] J. F. Donoghue and G. Valencia, Phys. Rev. Lett. **58**, 451 (1987) [Erratum-ibid. **60**, 243 (1988)]; M. B. Gavela, F. Iddir, A. Le Yaouanc, L. Oliver, O. Pene and J. C. Raynal, Phys. Rev. D **39**, 1870 (1989); M. P. Kamionkowski, Phys. Rev. D **41**, 1672 (1990).

- [2] O. Antipin, G. Valencia, Phys. Rev. **D79** (2009) 013013. [arXiv:0807.1295 [hep-ph]]; S. K. Gupta, A. S. Mete, G. Valencia, Phys. Rev. **D80** (2009) 034013. [arXiv:0905.1074 [hep-ph]]; S. K. Gupta, G. Valencia, Phys. Rev. **D81** (2010) 034013. [arXiv:0912.0707 [hep-ph]].
- [3] D. Chang and W. Y. Keung, Phys. Lett. B **305**, 261 (1993) [arXiv:hep-ph/9301265]; J. F. Gunion, X. -G. He, Phys. Rev. Lett. **76**, 4468-4471 (1996). [hep-ph/9602226]; W. Bernreuther and A. Brandenburg, Phys. Lett. B **314**, 104 (1993); W. Bernreuther and A. Brandenburg, Phys. Rev. D **49**, 4481 (1994) [arXiv:hep-ph/9312210]; W. Bernreuther, A. Brandenburg and M. Flesch, arXiv:hep-ph/9812387; G. Valencia, Y. Wang, Phys. Rev. **D73** (2006) 053009. [hep-ph/0512127].
- [4] J. Berger, M. Blanke, Y. Grossman, JHEP **1108**, 033 (2011). [arXiv:1105.0672 [hep-ph]]; N. D. Christensen, T. Han, Y. Li, Phys. Lett. **B693**, 28-35 (2010). [arXiv:1005.5393 [hep-ph]]; G. Moortgat-Pick, K. Rolbiecki, J. Tattersall, P. Wienemann, JHEP **1001**, 004 (2010). [arXiv:0908.2631 [hep-ph]]; R. M. Godbole, D. J. Miller, 2, M. M. Muhlleitner, JHEP **0712**, 031 (2007). [arXiv:0708.0458 [hep-ph]].
- [5] K. Hagiwara, K. Mawatari and H. Yokoya, JHEP **0712**, 041 (2007) [arXiv:0707.3194 [hep-ph]].
- [6] A. V. Manohar, M. B. Wise, Phys. Rev. **D74**, 035009 (2006). [hep-ph/0606172].
- [7] M. I. Gresham, M. B. Wise, Phys. Rev. **D76**, 075003 (2007). [arXiv:0706.0909 [hep-ph]].
- [8] G. Aad *et al.* [ATLAS Collaboration], [arXiv:1108.6311 [hep-ex]]; S. Chatrchyan *et al.* [CMS Collaboration], Phys. Lett. **B704**, 123 (2011).
- [9] C. P. Burgess, M. Trott and S. Zuberi, JHEP **0909**, 082 (2009) [arXiv:0907.2696 [hep-ph]].
- [10] L. M. Carpenter and S. Mantry, arXiv:1104.5528 [hep-ph].
- [11] T. Stelzer and W. F. Long, Comput. Phys. Commun. **81**, 357 (1994) [arXiv:hep-ph/9401258]; J. Alwall *et al.*, JHEP **0709**, 028 (2007) [arXiv:0706.2334 [hep-ph]]; J. Alwall, M. Herquet, F. Maltoni, O. Mattelaer, T. Stelzer, JHEP **1106**, 128 (2011). [arXiv:1106.0522 [hep-ph]].
- [12] J. Pumplin, D. R. Stump, J. Huston, H. L. Lai, P. M. Nadolsky and W. K. Tung, JHEP **0207**, 012 (2002) [arXiv:hep-ph/0201195].
- [13] S. Weinberg, Phys. Rev. **D42**, 860-866 (1990).
- [14] M. Spira, A. Djouadi, D. Graudenz, P. M. Zerwas, Nucl. Phys. **B453**, 17-82 (1995). [arXiv:hep-ph/9504378 [hep-ph]].